

Computation of the Alpha Cabin sound absorption coefficient by using the finite transfer matrix method (FTMM): inter-laboratory test on porous media

Andrea Santoni

Engineering Department, University of Ferrara, via G. Saragat 1, 44122 Ferrara, Italy
Email: andrea.santoni@unife.it

Paolo Bonfiglio

Materiacustica srl, via C. Ravera, 15/A, 44122 Ferrara, Italy
Email: paolo.bonfiglio@materiacustica.it

Patrizio Fausti

Engineering Department, University of Ferrara, via G. Saragat 1, 44122 Ferrara, Italy
Email: patrizio.fausti@unife.it

Francesco Pompoli

Engineering Department, University of Ferrara, via G. Saragat 1, 44122 Ferrara, Italy
Email: francesco.pompoli@unife.it

ABSTRACT

The transfer matrix method (TMM) has become an established and widely used approach to compute the sound absorption coefficient of a multilayer structure. Due to the assumption made by this method of laterally infinite media, it is necessary to introduce in the computation the finite-size radiation impedance of the investigated system, in order to obtain an accurate prediction of the sound absorption coefficient within the entire frequency range of interest; this is generally referred to as finite transfer matrix method (FTMM). However, it has not been extensively investigated the possibility of using the FTMM to accurately approximate the sound absorption of flat porous samples experimentally determined in an Alpha Cabin, a small reverberation room employed in the automotive industry. To this purpose, a simulation-based round robin test was organised involving academic and private research groups. Four different systems constituted by five porous materials, whose properties were experimentally characterised, were considered. Each participant, provided with all the mechanical and physical properties of each medium, was requested to simulate the sound absorption coefficient with an arbitrary chosen code, based on the FTMM. The results indicated a good accuracy of the different formulations to determine the finite-size radiation impedance. However, its implementation in the computation of the sound absorption coefficient, as well as the upper limit of the range of incidence angles within which the acoustic field is simulated, and the model adopted to describe each material, significantly influenced the results.

Keywords: sound absorption; transfer matrix method; finite size correction; radiation impedance; Alpha Cabin

1 Introduction

The transfer matrix method (TMM) has become an established approach used to compute the sound absorption coefficient as well as the sound transmission loss of a given multilayer system. However, it is well known that a reliable characterisation of the materials' properties is a necessary but not sufficient condition to guarantee that the computed diffused sound absorption coefficient accurately approximates, within the entire frequency range of interest, the results measured in a reverberant chamber, according to the standards ISO 354 [1] or ASTM C423 [2]. In fact, it is also necessary to apply a correction to take into account the finite size of the samples [3], as explained in Chapter 12 of reference [4]. This is done by introducing into the computation the radiation impedance of the investigated structure, which depends on its geometry, on the angle of incidence of the impinging sound wave, and possibly on the propagation direction of the structural wave. Different reliable formulations to compute such radiation impedance can be found in the literature. ISO 354 is the international reference standard for random incidence sound absorption measurements, performed in a reverberant room with a volume generally between 200 m^3 and 250 m^3 . Random incidence sound absorption measurements are significantly affected by the degree of diffusiveness of the sound field in the reverberant room. In fact, the assumption of a perfectly diffused omnidirectional sound field, on which the sound absorption measurement is based, might not occur within the entire frequency range, especially when the testing sample is inside the room [5]. Moreover, at the lower frequencies, the measured sound absorption can also be overestimated due to the sample's edge effect [6, 7]. Although these aspects can affect even more significantly measurements made in small rooms, there is a growing interest in the use of smaller test facilities to evaluate the sound absorption coefficient of porous materials in many industrial fields [8]. The so called Alpha Cabin is a smaller reverberation room, which has been largely utilised in the automotive industry for the measurement of acoustic absorption properties of materials and components employed in noise control and sound insulation of vehicles. The Alpha Cabin test facility is significantly smaller than a standard reverberation room, with a volume varying approximately between 6 and 7 m^3 . Some studies have investigated the possibility to accurately predict sound absorption measured in an Alpha Cabin using the TMM approach [9, 10]. Nevertheless, to the best of our knowledge, at the moment there is no evidence that the finite-size correction is also suitable to accurately approximate the sound absorption of flat porous samples experimentally determined in the Alpha Cabin test rig. To this purpose, four different rectangular and planar systems were tested in the Alpha Cabin originally developed by Rieter, a Swiss company based in Winterthur. Moreover, their elastic characteristics and their physical parameters were experimentally determined in the Acoustic Laboratory of the University of Ferrara. In order to extend this study to different commercial or in-house implemented codes, we asked academic and private acoustic research groups to compute the random incidence sound absorption coefficient of such systems, with the provided acoustic, elastic and physical properties of each material considered. In the next section, the basic concepts of the transfer matrix method and the finite-size radiation impedance are recalled, and the different models used to describe wave propagation in porous materials are presented. In section 3, the investigated systems are described and the research groups which took part to this inter-laboratory test are introduced. The results are presented and discussed in section 4. Finally, conclusions are drawn in section 5.

2 Sound absorption measurements and computation

2.1 Alpha Cabin measurements

The random incidence sound absorption coefficient of four porous systems, introduced in section 3, was experimentally evaluated in an Alpha Cabin. This small reverberation chamber with non-parallel walls has a volume of 6.44 m³ and maximum reverberation time equal to 2.5 s. It was originally developed as a dimensional scale reduction of 1:3 of the full-size reverberation room at the Swiss Laboratory of Material Testing and Research Institute (EMPA) in Dübendorf. The cabin is equipped with diffusing curved panels hanging from the lateral walls, and a conic-shaped diffuser mounted on the ceiling, as shown in Fig. 1. The sound field inside the Alpha Cabin is generated by the three loudspeakers, driven with either white

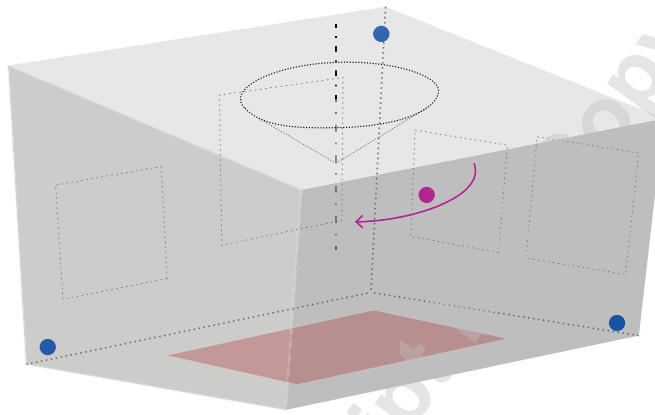


Fig. 1. Diagram of the Alpha Cabin used for the experimental investigation of the systems: the blue circles represent the position of the three sound sources; the purple circle represents the microphone; the red rectangle is the 1.2 m² sample.

noise bursts, or a sine sweep signal. The reverberation time is determined in one-third octave bands, by averaging over five different microphone positions equally spaced in a circle at a height of 90 cm from the floor, in the first case according to the interrupted noise method, in the latter by means of the integrated impulse response method. The volume of the cabin allows for a cut-off (or minimum) frequency of approximately 300 Hz, above which the acoustic field of the reverberation room has the potential to be diffused [11, 12]. Measurements are taken in one-third octave bands within the frequency range 400 Hz-10000 Hz. All the tested systems, with a surface of $S = 1.0\text{ m} \times 1.2\text{ m} = 1.2\text{ m}^2$, were inserted into a metal frame in order to reduce the border effects [13]. The same frame was left inside the cabin in order to determine the equivalent absorption area of the empty chamber. The sound absorption coefficient of the specimen tested in the Alpha Cabin is determined, consistently with the measurement in a normal-size reverberation room, from the classical formula based on Sabine's theory, with minor adjustments:

$$\alpha_s = 0.92 \left[0.163 \frac{V}{S} \left(\frac{1}{T_2} - \frac{1}{T_1} \right) \right] \quad (1)$$

where T_1 and T_2 are the Cabin reverberation times measured respectively without and with the specimen. It can be observed that Eq. (1), consistently with the current ISO 354, does not account for the fact that, with the specimen inside the room, it would be necessary to subtract the surface of the tested sample, in order to correctly compute the equivalent absorption area of the empty room. Unlike in ISO 354, the air contribution on sound absorption is not taken into account in Eq. (1). However, since the temperature in the cabin t and especially the relative humidity RH play a substantial role, it is important to maintain a stationary condition with $t \approx 18^\circ - 25^\circ$ and $RH \leq 50\%$ during the measurement (the recommended temperature range and relative humidity may slightly change according to the producer's manual). The correction factor equal to 0.92 was introduced in order to take the edge effect into consideration and to avoid the absorption coefficients obtained in the Alpha Cabin substantially exceeding 100%. Such a value was determined by comparing the Alpha Cabin sound absorption coefficient with the results obtained in Empa's full-scale reverberation room. According to the manual of the Alpha Cabin, a tolerance equal to ± 0.035 was found in the 500 Hz octave and about equal to ± 0.025 in the octave bands from 1000 Hz to 8000 Hz.

2.2 The Transfer Matrix Method framework

The transfer matrix method [14–16], (TMM) is a widely used computationally-efficient approach to investigate wave propagation in laterally infinite multilayer structures considering different media, such as elastic solids, rigid and elastic framed porous materials, membranes, resonators, porous and impervious screens. Considering an acoustic plane wave incident with an angle θ on the surface of the investigated structure, backed by a rigid wall, it is possible to calculate its sound absorption coefficient as

$$\alpha(\theta) = 1 - |R(\theta)|^2 = 1 - \left| \frac{Z_s(\theta) \cos \theta - Z_0}{Z_s(\theta) \cos \theta + Z_0} \right|^2 \quad (2)$$

where R is the complex reflection coefficient, Z_0 the characteristic impedance of the air and Z_s the surface acoustic impedance of the element, given by the ratio of the sound pressure to the particle velocity on the excited surface of the layered structure. The surface acoustic impedance Z_s is determined by the global transfer matrix which describes wave propagation through the layered structure. The size of this matrix depends on the number of layers this structure consists of and on their nature. The sound absorption coefficient is dependent upon the angle of incidence θ of the impinging plane wave. The sound absorption coefficient for a diffused sound field excitation can be computed as

$$\alpha_d = \frac{\int_0^{\pi/2} \alpha(\theta) \cos \theta \sin \theta d\theta}{\int_0^{\pi/2} \cos \theta \sin \theta d\theta} \quad (3)$$

Due to the assumption of laterally infinite media, deviation between predicted and experimental absorption coefficient is usually found at low frequencies. In order to increase the accuracy of the results, the finite-size radiation impedance to

airborne excitation $Z_R(\theta, \phi)$ is introduced in the computation, which depends on both the incidence angle of the acoustic wave θ and the azimuthal angle on the structure's plane ϕ . However, in case of isotropic media, this can be replaced by $Z_{R,avg}(\theta)$: its average over the azimuthal angle ϕ . Introducing the finite-size correction, the diffuse field incidence sound absorption coefficient can be expressed as

$$\alpha_d = \frac{\int_0^{\pi/2} \frac{4\Re\{Z_s(\theta)\}}{|Z_s(\theta) + Z_{R,avg}(\theta)|^2} \sin \theta d\theta}{\int_0^{\pi/2} \cos \theta \sin \theta d\theta} \quad (4)$$

The application of the finite-size correction to the transfer matrix framework, which introduces the radiation impedance Z_R , is generally referred to as finite transfer matrix method (FTMM) [17]. According to chapter 12 of [4], a 'true' absorption coefficient can be computed by taking into account the geometric impedance seen by the incident wave as

$$\alpha_{d,(true)} = \frac{\int_0^{\pi/2} \frac{4\Re\{Z_s(\theta)\}}{|Z_s(\theta) + Z_{R,avg}(\theta)|^2} \sin \theta d\theta}{\int_0^{\pi/2} \frac{4}{|1 + Z_{R,avg}(\theta) \cos \theta|^2} \cos \theta \sin \theta d\theta} \quad (5)$$

The radiation impedance of a rectangular vibrating structure, with a and b indicating its length and width, is defined as

$$Z_R(\theta, \phi) = \int_0^a \int_0^b \int_0^{a'} \int_0^{b'} w_n(x, y) G(x, y, x', y') w_n^*(x', y') da db da' db' \quad (6)$$

where w_n is the plate's vibrational field distribution, the superscript $*$ indicates the complex conjugate and G represents the half-space Green's function:

$$G(x, y, x', y') = e^{jk_0 R} (2\pi R)^{-1} \quad (7)$$

where $R = \sqrt{(x - x')^2 + (y - y')^2}$ and k_0 the acoustic wavenumber. Different reliable formulations to compute the finite-size radiation impedance can be found in the literature. A thorough review of most of these different approaches was presented by Bonfiglio et al. [3], related to both sound absorption coefficient and sound transmission loss [18]. Nevertheless, all the formulations, considered in this inter-laboratory test, are briefly summarised below. Thomasson [19, 20] investigated the relationship between the size of the sample and the absorption coefficient, and derived, by means of a variational approach, a specific radiation impedance to take into account the influence of the finite geometry of the panel. Villot et al. [21, 22] proposed a spatial-windowing technique to take into account the structure's dimensions in sound transmission and sound radiation problems, deriving a formulation for the real part of the normalised radiation impedance (i.e. the radiation efficiency)

within the wavenumber domain. Vigran [23] proposed a one-dimensional simplification based on the spatial windowing approach for sound transmission problems through isotropic materials. Even though this formulation was specifically derived to be applied to sound transmission computation, it was somehow implemented in a commercial software based on the TMM framework to also take into account the finite-size of the specimen in sound absorption problems. Unfortunately, further details are not available in the manual. Ghinet and Atalla [24] proposed a general expression for radiation impedance based on the Rayleigh integral. The main drawback of this approach is its high computational cost. Rhazi and Atalla [25] presented an analytical derivation to implement a more efficient formulation. Moreover, a faster and accurate formulation to compute the radiation impedance was proposed by Bonfiglio et al. [3], although, similarly to the approaches proposed by Thomasson and Vigran, it requires that the structure's aspect ratio be not far from a square one, and it cannot be applied to orthotropic media. These are the models, available in commercial software or in-house implemented codes, which we were able to compare in the inter-laboratory test presented here.

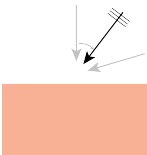
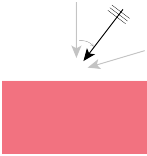
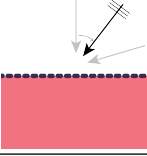
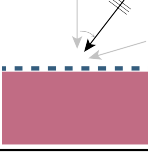
2.3 Modelling sound propagation in porous media

Within the TMM framework, introduced in section 2, acoustical porous media can be modelled as equivalent-fluids, considering a rigid and motionless frame. To this purpose, Delany and Bazley [26] developed an empirical model which only requires the thickness of the sample h and the material airflow resistivity σ as input data. Miki [27, 28] modified this model, introducing two more physical parameters: the open porosity ϕ and the tortuosity α_∞ . Several models were developed in order to investigate different fibrous, porous or granular materials. One of the most used and implemented in commercial software is the equivalent fluid model commonly known as Johnson-Champoux-Allard (JCA), which takes into account both the visco-inertial effects [29] and the thermal effects [30]. This model, introducing the viscous and thermal characteristic lengths Λ and Λ' , is based on five physical parameters. The JCA equivalent fluid model can also be used for limp materials, taking into account an additional parameter, represented by the equivalent effective density ρ_{limp} , to consider the inertia of the frame [31]. Besides, perforated plates and screens can also be easily modelled as a porous medium [32]. The equivalent fluid simplification, which assumes that the solid frame is motionless, can be used for frequencies above the decoupling frequency, since, due to the weak coupling between the solid and the fluid phase, the acoustic wave will induce negligible vibration in the solid frame [4]. Below this frequency limit, it is necessary to adopt a poro-elastic model, which considers wave propagation both in the elastic frame and in the fluid saturating the open pores, by means of Biot's theory [33, 34]. The fluid phase is described by the 5 parameters of the JCA model. In addition, the properties characterising the solid frame are also required; these are the sample's density ρ , the material elastic modulus E , its loss factor η and Poisson ratio ν . Bécot and Jaouen [35] derived Biot's equations for any acoustic model.

3 Materials and participants

The random incidence sound absorption coefficient of four different porous systems, shown in Table 1, was tested in an Alpha Cabin. System #A was a 16 mm thick single layer of a micro-fibre material; system #B was an 11 mm layer of a thermoplastic fibrous material; system #C was realised by coupling the same thermoplastic material as system #B

Table 1. Models used by each participant to characterise the porous materials of the four tested systems.

System	Mat.	G01	G02	G03	G04	G05	G06	G07
#A 	1	JCA	JCA	JCA	Miki	JCA	JCA limp	JCA limp
#B 	2	Biot	Biot	Biot	Miki	Biot	Biot	JCA limp
#C 	3 2	JCA ¹ - DB Biot	JCA ¹ Biot	JCA ¹ Biot	- Miki	JCA ¹ Biot	JCA ¹ Biot	Porous facing JCA limp
#D 	5 4	Biot Biot	Biot Biot	Biot Biot	-	Biot Biot	Biot Biot	JCA limp JCA limp

with a resistive screen, constituted by a woven fabric layer, glued on the receiving side; system #D was composed of a different 17 mm thick thermoplastic material covered with a perforated aluminium foil. All the elements were planar and rectangular, with a length of 1.2 m and a width of 1.0 m. The mechanical characteristics and the physical parameters of these five materials were experimentally determined in the Acoustic Laboratory of the University of Ferrara and they are provided in Table 2. The experimental characterisation of all the properties of each material ensured the reliability of the input data used to evaluate the sound absorption coefficient of the four systems. More specifically, the airflow resistivity σ of materials n. 1, 2 and 4 was measured according to the alternating flow method, described in the standard ISO 9053 [37]². The porosity ϕ of these materials was measured according to the experimental procedure described in reference [38], based on the isothermal compression of a give volume of air in which the sample of porous material is immersed [39]. Their tortuosity α_∞ was experimentally assessed by means of ultrasonic tests [40]. The viscous and thermal characteristic lengths Λ and Λ' were evaluated according to an established inversion technique [41]. When required, the materials' elastic properties were determined through quasi-static uni-axial compression measurements [42]. The resistive screen layer, representing material n. 3 in Table 2, was tested in an impedance tube with an air gap of 100 mm. Its airflow resistivity and its porosity were determined according to the analytical approach proposed by Jaouen et al. [36]. The same approach was also used to characterise the JCA parameters for the perforated aluminium foil (material n. 5 in Table 2), while its elastic properties were taken from the literature.

As presented in the next section, the model's accuracy was assessed by comparing the predicted results with the sound

¹The 5 parameters required for the JCA model were obtained according to the procedure proposed in ref. [36]

²It was substituted by the standard ISO 9053-1: 2018 – Acoustics – Determination of airflow resistance Static airflow method, in which this method was not included. Even though the alternating flow approach still be considered a scientifically reliable experimental method.

Table 2. Mechanical and acoustic properties of the considered materials (experimentally evaluated).

Material	Geometry		Elastic Properties			Physical Parameters				
	h [mm]	ρ [kg/m ³]	E [Pa]	η [-]	ν [-]	σ [Ns/m ⁴]	ϕ [-]	α_∞ [-]	Λ [μ m]	Λ' [μ m]
1	16	34	-	-	-	19694	0.98	1.05	78	107
2	11	128	1.60E+05	0.15	0.05	115680	0.93	1.10	25	50
3	1	-	-	-	-	680000	0.70	-	-	-
4	17	103	1.04E+05	0.12	0.02	26069	0.95	1.10	70	90
5	1	2600	6.30E+10	0.01	0.33	178000	0.06	1.00	250	250

absorption measured in the Alpha Cabin. In order to extend our study to different commercial or in-house implemented codes, we asked seven different academic and private acoustic research groups to compute the random incidence sound absorption coefficient of such systems, as mentioned above. We provided each participant with the mechanical and physical properties, as given in 2, together with the system's geometry, without further indications nor limitations. Each participant was able to decide which model should be used to describe each layer and the formulation to evaluate the finite-size radiation impedance, according to the possibilities offered by the software, either an in-house implemented code or a commercial one. In order to respect the privacy of all the participants, the collected data are presented in anonymous form; both the identity of the participants and the name of the software used are undisclosed. Nevertheless, the characteristics of each code employed are summarized in Table 3, specifying for each participant whether a commercial software or an in-house implemented code was used, the model adopted for each layer and which formulation was implemented to take into account the finite-size radiation impedance of the system.

4 Results and discussion

Fig. 2 shows the comparison, in one-third octave bands, between the numerical results provided by each participant group and the experimental sound absorption coefficient of system #A $\alpha_{Exp,S\#A}$, measured in the Alpha Cabin. In particular, in Fig. 2 a), $G_{i,FTMM,-j}$ represents the results computed by the j^{th} group with an FTMM-based code, evaluating the geometrical radiation impedance Z_R according to the j^{th} model, as indicated in Table 3. These results were obtained considering the angle of incidence of the acoustic impinging plane wave within the range $0 \leq \theta \leq 90^\circ$. In Fig. 2 b) the average sound absorption $\alpha_{avg,FTMM}$, computed from the results given in the left-hand side graph, is compared with the experimental results. The average sound absorption is plotted as a black dashed line, while the shaded area represents the maximum positive and negative deviation found for each third octave band, computed as $\epsilon^+ = \max(\alpha_{G_{i,FTMM,-j}} - \alpha_{avg,FTMM})$ and $\epsilon^- = \max(\alpha_{avg,FTMM} - \alpha_{G_{i,FTMM,-j}})$. The chart also shows the results computed without considering the finite-size of the structure, indicated with the subscript TMM . Moreover, some of the participants also provided the sound absorption computed using a limited range of the incidence angle $0 < \theta < 78^\circ$, often referred to as field incidence. This is indicated with the sub-

Table 3. Specification of the software used by each participant.

	Software	Available Medium Models	Radiation Impedance Model
Group 1	In-house implemented	Elastic Solid Delany-Bazley Johnson-Champoux-Allard Poroelastic	Bonfiglio et al. - B
Group 2	In-house implemented	Elastic Solid Delany-Bazley Johnson-Champoux-Allard Poroelastic	Bonfiglio et al. - B
Group 3	Commercial (s ₁)	Johnson-Champoux-Allard Poroelastic	Rhazi et al. - R
Group 4	In-house implemented	Miki	Thomasson - T
	a) Commercial (s ₂)	Delany-Bazley Johnson-Champoux-Allard Poroelastic	None
	b) Commercial (s ₃)	Delany-Bazley Miki Johnson-Champoux-Allard Poroelastic	Not Specified - NS
Group 5			
	c) Commercial (s ₄)	Elastic Solid Delany-Bazley Miki Johnson-Champoux-Allard Johnson-Champoux-Allard-Lafarge Poroelastic Others	Rhazi et al. - R Thomasson - T
		Elastic Solid Delany-Bazley Miki	Rhazi et al. - R
Group 6	Commercial (s ₄)	Johnson-Champoux-Allard Johnson-Champoux-Allard-Lafarge Poroelastic Others	Thomasson - T Bonfiglio et al. - B
Group 7	Commercial (s ₄)	Elastic Solid Delany-Bazley Johnson-Champoux-Allard Johnson-Champoux-Allard limp	Vigran - V

script $\theta_{max=78^\circ}$. Finally, the results computed considering the *true* formulation, given in Eq. (5) are also provided, indicated with the subscript $FTMM-j(true)$. The analogous comparisons associated to systems #B, #C and #D, are given in Fig. 3, Fig. 4 and Fig. 5 respectively. The comparisons on the left-hand side graphs of Figures 2 to 5 showed a general good agreement of all the results obtained with the FTMM, according to Eq. (4), and the experimental sound absorption coefficient. However, it is worth investigating some of the discrepancies found. It can be observed that the results are significantly affected by the model employed to describe the porous materials. Group 4 modelled material n. 1 as an equivalent fluid, according to Miki's model, while the other groups applied the standard or the limp JCA model. Consistently, the thermoplastic fibrous material employed in system #B (medium n. 2 in Table 2) was modelled as a poro-elastic medium by all the participants except Group 4 and Group 7; they described the material as an equivalent fluid: the former used again Miki's model, while the latter

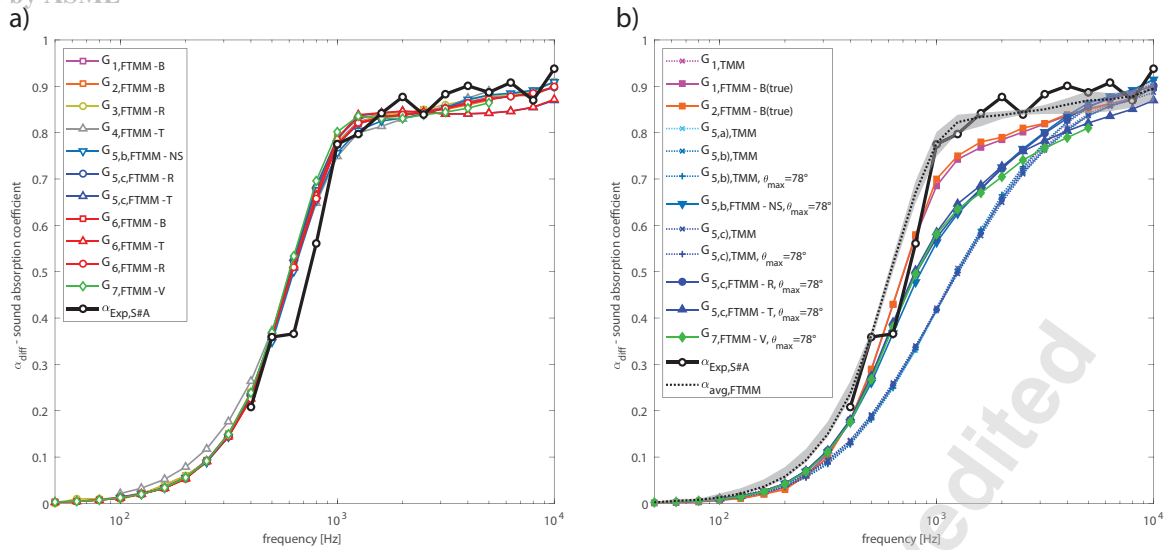


Fig. 2. Sound absorption coefficient of System #A - comparison between numerical and experimental data: a) the FTMM results are computed considering the finite-size radiation impedance and the angle of incidence in the range $0 \leq \theta \leq \pi/2$; b) comparison between the arithmetic average of the FTMM data and the results computed with some TMM variations.

the limp JCA model, which caused a slight overestimation of the sound absorption below 1000 Hz, as can be observed in Fig. 3 a). The influence of the model employed to describe wave propagation through the porous media is also shown in

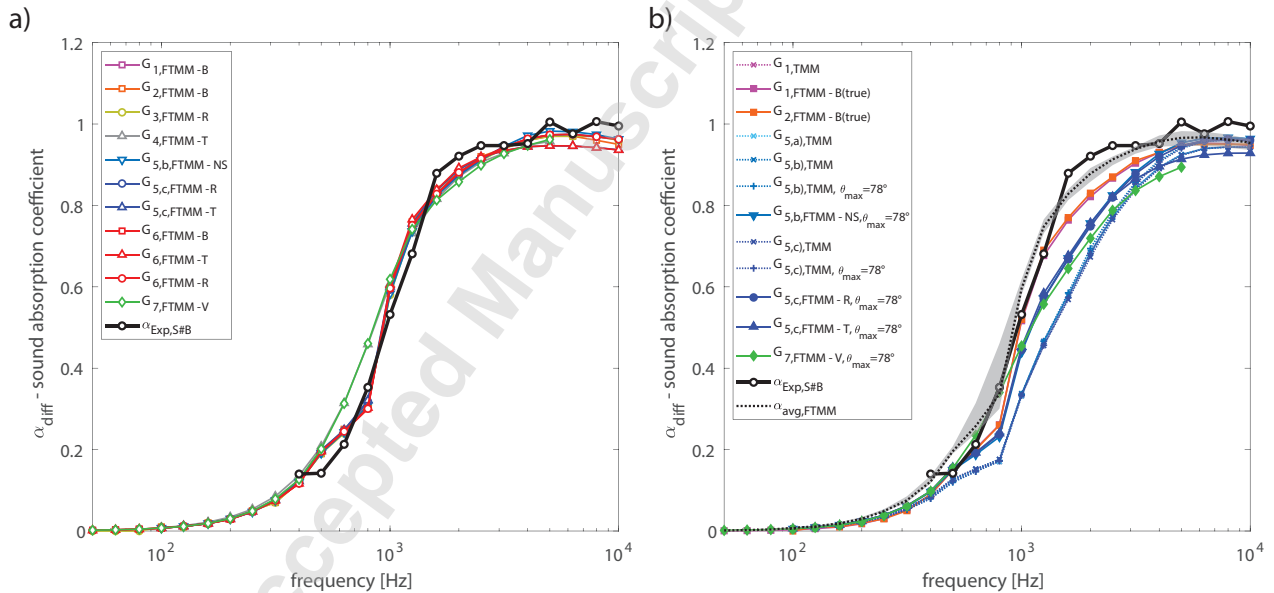


Fig. 3. Sound absorption coefficient of System #B - comparison between numerical and experimental data: a) the FTMM results are computed considering the finite-size radiation impedance and the angle of incidence in the range $0 \leq \theta \leq \pi/2$; b) comparison between the arithmetic average of the FTMM data and the results computed with some TMM variations.

Fig. 4. All the participants, except Group 7, modelled the resistive screen layer of system #C (Material n. 3 in Table 2) as an equivalent fluid, using the JCA model, and the thermoplastic fibrous layer as a poro-elastic medium. Group 7, on the other

hand, adopted the porous facing model proposed by Rebillard [43] to describe the resistive screen, and the limp JCA model to describe the thermoplastic material, leading to slightly different results below 1250 Hz. A further example is represented by the additional results provided by Group 1, in which the resistive screen layer was alternatively described using the model developed by Delany and Bazley rather than the JCA model. The obtained results, indicated introducing the subscript ($_{DB}$), slightly overestimated the absorption coefficient at low frequencies and underestimated it above 1000 Hz. Consistent effects were also shown by the results computed without taking into account the finite-size correction, presented in Fig. 4 b), which will be further discussed later in this section. The step observed in the experimental sound absorption between the 500 Hz and the 630 Hz frequency bands, as well as the consequent deviation of the simulated results up to 1600 Hz may be caused by an increase in the screen layer's stiffness due to the gluing over the porous material. For this reason, it would probably be more appropriate to describe the glued screen using the poro-elastic model. However, the characterisation of its elastic properties is impractical. A remarkably good agreement was shown between all the FTMM results and the experimental

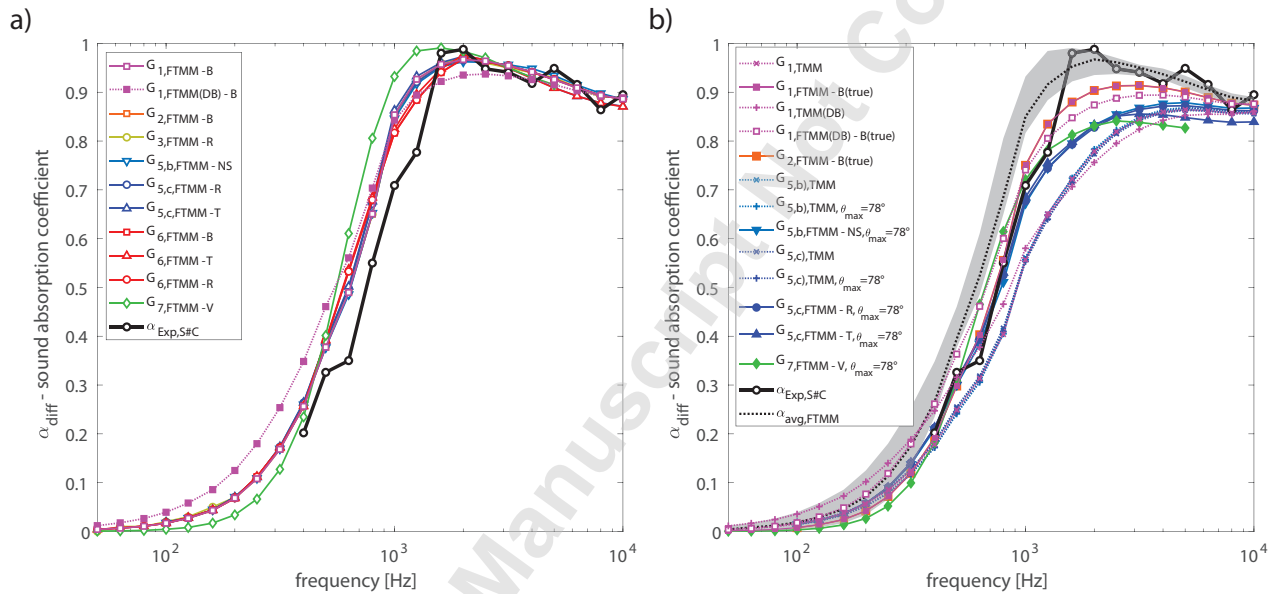


Fig. 4. Sound absorption coefficient of System #C - comparison between numerical and experimental data: a) the FTMM results are computed considering the finite-size radiation impedance and the angle of incidence in the range $0 \leq \theta \leq \pi/2$; b) comparison between the arithmetic average of the FTMM data and the results computed with some TMM variations.

data for system #D, shown in Fig. 5 a), regardless of the models adopted to characterise the porous media or the formulation which was used to evaluate the finite-size radiation impedance. Generally, all the formulations considered to evaluate the finite-size radiation impedance provided similar results, allowing for a good approximation of the sound absorption coefficient measured in the Alpha Cabin. Only minor differences associated with the formulation employed could be observed: results computed using Thomasson's formulation underestimated the sound absorption coefficient at high frequencies, for systems #A and #B and, to a lesser extent, also for systems #C and #D.

In the graphs on the right-hand side of Figures 2 to 5, the sound absorption averaged over all the FTMM results just

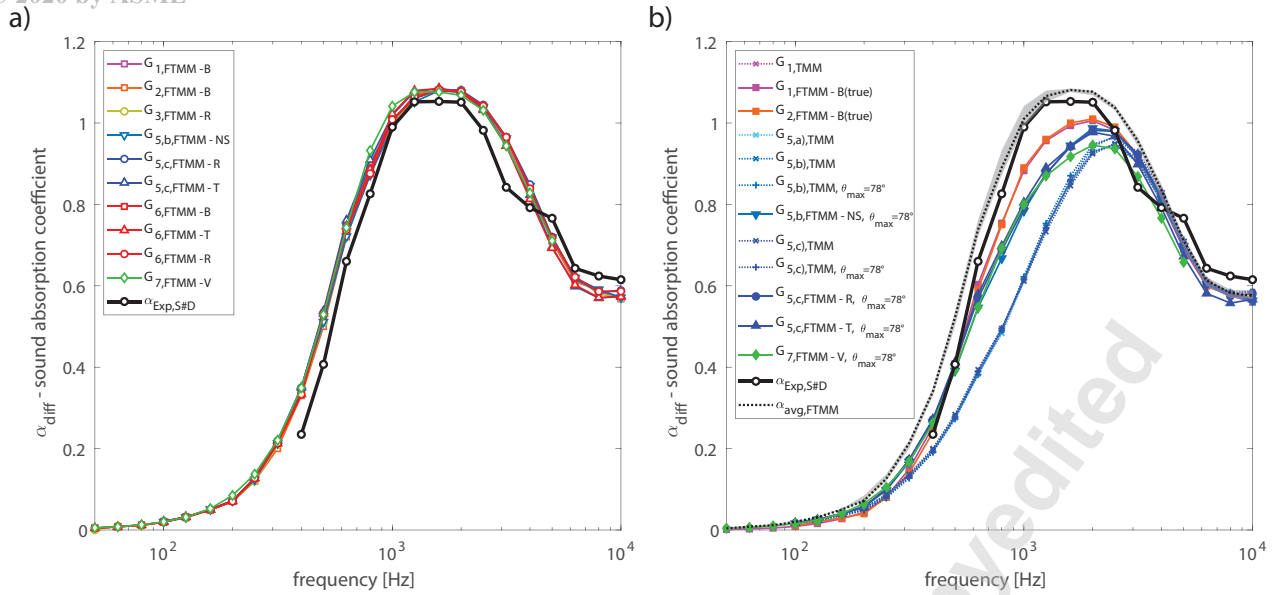


Fig. 5. Sound absorption coefficient of System #D - comparison between numerical and experimental data: a) the FTMM results are computed considering the finite-size radiation impedance and the angle of incidence in the range $0 \leq \theta \leq \pi/2$; b) comparison between the arithmetic average of the FTMM data and the results computed with some TMM variations.

discussed and the associated deviation were compared with the experimental data and with the results obtained from some kind of variation in the TMM approach. For all the investigated systems a general good agreement could be observed between the standard TMM results, which, as expected, underestimated the experimental data, due to the infinite size assumption. Significant differences were only found in system #C, when the resistive screen layer was modelled using the Delany and Bazley model rather than the JCA one. Only small differences were found when the TMM computation was applied to a limited angle of incidence, within the range $0 < \theta < 78^\circ$. A small improvement could be observed when this limitation was combined with the introduction of finite-size radiation, even though this approach still does not allow to correctly approximate the experimental sound absorption coefficient. Moreover, it should be noted that for all the systems, the *true* formulation to compute sound absorption coefficient, given in Eq. (5), provided an underestimation of the experimental results, even though the finite size of the samples was considered.

Finally, Fig. 6 shows the difference between the average sound absorption computed by means of the FTMM and the experimental data measured for each system in the Alpha Cabin. The error bars represent the standard deviation associated with the average FTMM sound absorption $\alpha_{avg,FTMM}$. With an expected error of around 5%, at high frequencies, a general good accuracy could be achieved predicting the Alpha Cabin sound absorption by means of the FTMM, for all the systems. For system #B a similar deviation was found also at lower frequencies. A good accuracy within the entire frequency range was also found for system #D. The larger errors, around 10%, are found in the low frequency range, while they drop down to 5% at higher frequencies, except for the band centred around 3150 Hz, where the experimental sound absorption exhibits a rapid reduction. On the other hand, a significantly larger deviation was found in some mid-frequency third-octave bands for systems #A and #C. For the former, errors of 15% and 10% were found, between the average FTMM results and the Alpha Cabin sound absorption, in the bands centred around 630 Hz and 800 Hz respectively. For system #C, a deviation of

approximately 17% was found in the 630 Hz band and around 15% in the frequency range between 800 Hz - 1250 Hz. For these two systems, the higher standard deviation between the FTMM results was also found. It should be mentioned that in a three-year round robin test on sound absorption measurements in reverberant rooms with a different size [11,44,45], similar, or in some cases even larger, deviations were observed between the sets of data measured in various Alpha Cabin test-rigs, which were all qualified according to the OEM standard.

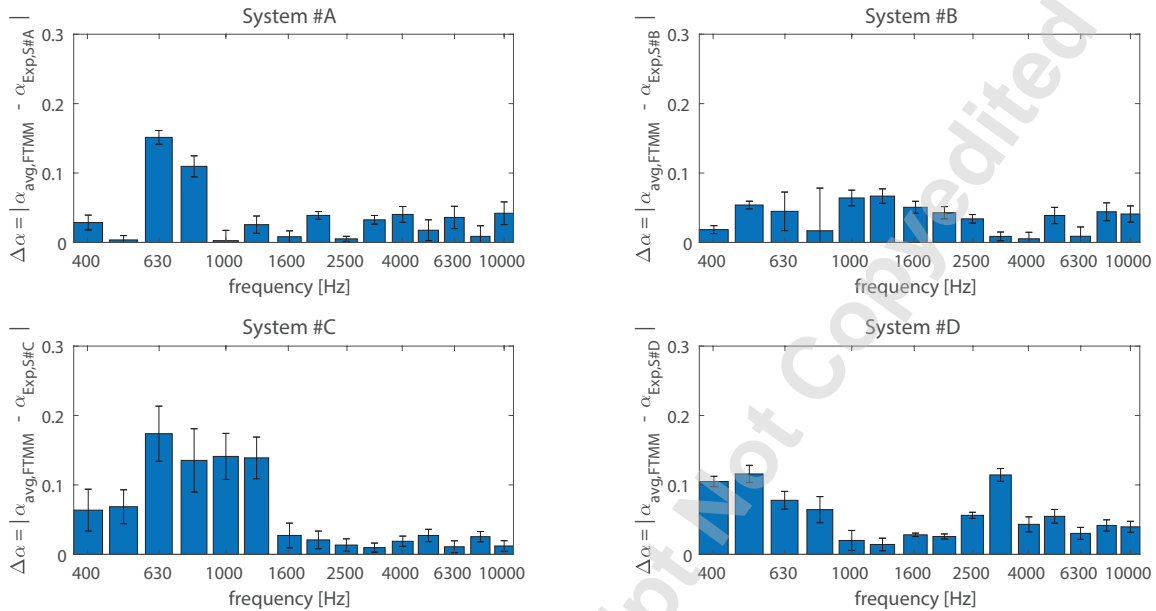


Fig. 6. Mean difference between the experimental sound absorption coefficient measured in the Alpha Cabin and the results predicted with the FTMM. The error bars represent the standard deviation associated with the arithmetic average of the FTMM results.

5 Conclusions

In this paper the reliability of the FTMM was analysed to compute the sound absorption coefficient of rectangular planar poro-elastic systems measured in an Alpha Cabin test rig. In order to compare the most relevant formulations to evaluate the finite-size radiation impedance, and the different approaches to describe the porous materials, an inter-laboratory test was organised involving both academic and private research groups. Two different fibrous materials and two systems, constituted by a layer of fibrous material lined with a resistive screen, were selected to represent typical sound absorbing components found in the automotive industry. It was observed that all the investigated formulations to compute the finite-size radiation impedance produced a good approximation of the diffuse incidence sound absorption measured in an Alpha Cabin. In fact, a small deviation was found between the results provided by the participants and computed with different software. The comparison between the sound absorption averaged over all the FTMM results and the experimental results highlighted a good accuracy of the model. At high frequencies a maximum deviation of about 5% was found, while below 1500 Hz a larger error, up to 15%-20%, could be expected for systems involving a resistive screen. The FTMM can definitely be used as a

reliable tool to accurately predict the Alpha Cabin sound absorption, when correctly implemented and assuming a reliable set of input data is available. In fact, the results presented showed significant differences, according to the model chosen to represent the porous media, or based on the maximum incidence angle considered for the impinging acoustic plane wave. Based on the findings presented in this paper, a few simple recommendations can be defined in order to implement an FTMM model to accurately compute the sound absorption coefficient measured in a small or a full size reverberant room:

1. the finite-size radiation impedance must be considered, by using, for example, one of the different formulations which were compared in this study, for which no significant differences were observed;
2. the finite-size radiation impedance has to be included in the computation according to Eq. (4). In fact, taking into account the finite-size effect also in the incidence sound power, as expressed by Eq. (5), leads to underestimated results;
3. a diffuse sound field needs to be considered, by sweeping the angle of incidence of the acoustic plane wave impinging on the system within the range $0 < \theta < \pi/2$ rad. Limiting it to the field incidence $0 < \theta < 0.43\pi$ rad ($\approx 78^\circ$) leads to an underestimation of the sound absorption coefficient;
4. it is important to evaluate which is the more appropriate model to describe a given porous material. In fact, when the equivalent fluid model is adopted for relatively heavy and stiff material, neglecting the elasticity of the solid frame causes an overestimation of the sound absorption in the mid-frequency range. In these cases, the poro-elastic model based on Biot's theory is more appropriate;
5. a resistive screen can be modelled as an equivalent fluid medium. The data indicated a better accuracy provided by the JCA model compared to the model developed by Delany and Bazley or the porous facing model proposed by Rebillard.

Acknowledgements

We would like to express our gratitude to all the research groups and the individuals who took part to this inter-laboratory test and made this study possible: Catherine Guigou-Carter (CSTB), Maurizio Tarello, Massimiliano Tiengo and Evan Harry (Adler Pelzer Group), Cheol-Ho Jeong (DTU), Lars Bischoff and Ludovic Dejaeger (Faurecia), François-Xavier Bécot (Matelys - Research Lab), Tor Erik Vigran (NTNU). They made it possible to compare and analyse results computed with different codes: AcouSYS software developed by CSTB, AlphaCell v11-2019 software developed by Matelys, DTU in-house implemented code, Maine 3A software ver. 1.5 developed by CTTM, NorFlag 4.0 software developed by T. E. Vigran and distributed by Norsonic, NOVA 2015 software from ESI Group, Protein in-house implemented code by Adler Pelzer Group, other than the in-house code implemented by the Acoustic Research Group of the University of Ferrara. We would also like to express our gratitude to François-Xavier Bécot for the critical analysis and the fruitful discussion about this work.

References

- [1] ISO 354:2003, 2003. Acoustics – Measurement of sound absorption in a reverberation room. Standard, International Organization for Standardization, Geneva, CH.
- [2] ASTM C423-17, 2017. Standard Test Method for Sound Absorption and Sound Absorption Coefficients by the Reverberation Room Method. Standard, ASTM International, West Conshohocken, PA, USA.
- [3] Bonfiglio, P., Pompoli, F., and Lioni, R., 2016. “A reduced-order integral formulation to account for the finite size effect of isotropic square panels using the transfer matrix method”. *The Journal of the Acoustical Society of America*, **139**(4), pp. 1773–1783.
- [4] Allard, J., and Atalla, N., 2009. *Propagation of sound in porous media: modelling sound absorbing materials*, 2nd ed. John Wiley & Sons, Ltd, Chichester, UK.
- [5] Nolan, M., Fernandez-Grande, E., Brunskog, J., and Jeong, C.-H., 2018. “A wavenumber approach to quantifying the isotropy of the sound field in reverberant spaces”. *The Journal of the Acoustical Society of America*, **143**(4), pp. 2514–2526.
- [6] Jeong, C.-H., 2013. “Converting sabine absorption coefficients to random incidence absorption coefficients”. *The Journal of the Acoustical Society of America*, **133**(6), pp. 3951–3962.
- [7] Jeong, C.-H., and Chang, J.-H., 2015. “Reproducibility of the random incidence absorption coefficient converted from the sabine absorption coefficient”. *Acta Acustica united with Acustica*, **101**(1), pp. 99–112.
- [8] Shtrepi, L., and Prato, A., 2020. “Towards a sustainable approach for sound absorption assessment of building materials: Validation of small-scale reverberation room measurements”. *Applied Acoustics*, **165**, p. 107304.
- [9] Bécot, F.-X., and Rodenas, J., 2016. “Predicting alpha cabin sound absorption in an industrial context”. In *INTER-NOISE and NOISE-CON Congress and Conference Proceedings*, Vol. 253. Hamburg, Germany, August 21–24, pp. 4648–4658.
- [10] Duval, A., Rondeau, J.-F., Dejaeger, L., Sgard, F., and Atalla, N., 2010. “Diffuse field absorption coefficient simulation of porous materials in small reverberant rooms: finite size and diffusivity issues”. In *Proceedings of the 10ème Congrès Française d’Acoustique*. Lyon, France, April 12–16.
- [11] Saha, P., Pan, J., and Veen, J. R., 2009. Thoughts behind Developing SAE Standard J2883-Random Incidence Sound Absorption Tests Using a Small Reverberation Room. Tech. rep., SAE Technical Paper 2009-01-2141.
- [12] Bertolini, C., and Guj, L., 2011. “Numerical simulation of the measurement of the diffuse field absorption coefficient in small reverberation rooms”. *SAE International Journal of Passenger Cars-Mechanical Systems*, **4**(2011-01-1641), pp. 1168–1194.
- [13] Chappuis, A., 1993. Small size devices for accurate acoustical measurements of materials and parts used in automobiles. Tech. rep., SAE Technical Paper 931266.
- [14] Lauriks, W., Mees, P., and Allard, J. F., 1992. “The acoustic transmission through layered systems”. *Journal of Sound and Vibration*, **155**(1), pp. 125–132.
- [15] Munjal, M. L., 1993. “Response of a multi-layered infinite plate to an oblique plane wave by means of transfer

matrices". *Journal of Sound and Vibration*, **162**(2), pp. 333–343.

- [16] Brouard, B., Lafarge, D., and Allard, J.-F., 1995. "A general method of modelling sound propagation in layered media". *Journal of Sound and Vibration*, **183**(1), pp. 129–142.
- [17] Atalla, N., Sgard, F., and Amedin, C. K., 2006. "On the modeling of sound radiation from poroelastic materials". *The Journal of the Acoustical Society of America*, **120**(4), pp. 1990–1995.
- [18] Santoni, A., Davy, J. L., Fausti, P., and Bonfiglio, P., 2020. "A review of the different approaches to predict the sound transmission loss of building partitions". *Building Acoustics*, **27**(3), pp. 253–279.
- [19] Thomasson, S.-I., 1980. "On the absorption coefficient". *Acta Acustica united with Acustica*, **44**(4), pp. 265–273.
- [20] Thomasson, S.-I., 1982. Theory and experiments on the sound absorption as a function of area. Tech. rep., Royal Institute of Technology, Stockholm, Sweden.
- [21] Villot, M., Guigou, C., and Gagliardini, L., 2001. "Predicting the acoustical radiation of finite size multi-layered structures by applying spatial windowing on infinite structures". *Journal of Sound and Vibration*, **245**(3), pp. 433–455.
- [22] Villot, M., and Guigou-Carter, C., 2005. "Using spatial windowing to take the finite size of plane structures into account in sound transmission". In *NOVEM Conference*. Saint Raphael, France, April 18-21.
- [23] Vigran, T. E., 2009. "Predicting the sound reduction index of finite size specimen by a simplified spatial windowing technique". *Journal of Sound and Vibration*, **325**(3), pp. 507–512.
- [24] Ghinet, S., and Atalla, N., 2001. "Sound transmission loss of insulating complex structures". *Canadian Acoustics*, **29**(3), pp. 26–27.
- [25] Rhazi, D., and Atalla, N., 2010. "A simple method to account for size effects in the transfer matrix method". *Journal of the Acoustical Society of America*, **127**(2), pp. EL30–EL36.
- [26] Delany, M., and Bazley, E., 1970. "Acoustical properties of fibrous absorbent materials". *Applied acoustics*, **3**(2), pp. 105–116.
- [27] Miki, Y., 1990. "Acoustical properties of porous materials - Modifications of Delany-Bazley models". *Journal of the Acoustical Society of Japan (E)*, **11**(1), pp. 19–24.
- [28] Miki, Y., 1990. "Acoustical properties of porous materials - Generalizations of empirical models". *Journal of the Acoustical Society of Japan (E)*, **11**(1), pp. 25–28.
- [29] Johnson, D. L., Koplik, J., and Dashen, R., 1987. "Theory of dynamic permeability and tortuosity in fluid-saturated porous media". *Journal of fluid mechanics*, **176**, pp. 379–402.
- [30] Champoux, Y., and Allard, J.-F., 1991. "Dynamic tortuosity and bulk modulus in air-saturated porous media". *Journal of applied physics*, **70**(4), pp. 1975–1979.
- [31] Panneton, R., 2007. "Comments on the limp frame equivalent fluid model for porous media". *The Journal of the Acoustical Society of America*, **122**(6), pp. EL217–EL222.
- [32] Atalla, N., and Sgard, F., 2007. "Modeling of perforated plates and screens using rigid frame porous models". *Journal of sound and vibration*, **303**(1-2), pp. 195–208.
- [33] Biot, M. A., 1956. "Theory of Propagation of Elastic Waves in a Fluid-Saturated Porous Solid. I. Low-Frequency

Range”. *The Journal of the Acoustical Society of America*, **28**(2), pp. 168–178.

[34] Biot, M. A., 1956. “Theory of propagation of elastic waves in a fluid-saturated porous solid. II. Higher frequency range”. *The Journal of the acoustical Society of america*, **28**(2), pp. 179–191.

[35] Bécot, F.-X., and Jaouen, L., 2013. “An alternative biot’s formulation for dissipative porous media with skeleton deformation”. *The Journal of the Acoustical Society of America*, **134**(6), pp. 4801–4807.

[36] Jaouen, L., and Bécot, F.-X., 2011. “Acoustical characterization of perforated facings”. *The Journal of the Acoustical Society of America*, **129**(3), pp. 1400–1406.

[37] ISO 9053:1991, 1991. Acoustics – Materials for acoustical applications – Determination of airflow resistance. Standard, International Organization for Standardization, Geneva, CH.

[38] Pompoli, F., and Bonfiglio, P., 2007. “Apparatus for measuring porosity open cell porous media (in italian)”. In *Proceedings of the 34th Acoustical Society of Italy National Conference*. Florence, Italy, June 13-15.

[39] Champoux, Y., Stinson, M. R., and Daigle, G. A., 1991. “Air-based system for the measurement of porosity”. *The Journal of the Acoustical Society of America*, **89**(2), pp. 910–916.

[40] Bonfiglio, P., and Pompoli, F., 2007. “Frequency dependent tortuosity measurement by means of ultrasonic tests”. In *Proceedings of the 14th International Congress on Sound and Vibration*, Vol. 14. Cairns, Australia, July 9-12, pp. 1–6.

[41] Bonfiglio, P., and Pompoli, F., 2013. “Inversion problems for determining physical parameters of porous materials: Overview and comparison between different methods”. *Acta Acustica united with Acustica*, **99**(3), pp. 341–351.

[42] Bonfiglio, P., Pompoli, F., Horoshenkov, K. V., Rahim, M. I. B. S. A., Jaouen, L., Rodenas, J., Bécot, F.-X., Gourdon, E., Jaeger, D., Kursch, V., Tarello, M., Roozen, N. B., Glorieux, C., Ferrian, F., Leroy, P., Briatico Vangosa, F., Dauchez, N., Foucart, F., Lei, L., Carillo, K., Doutres, O., Sgard, F., Panneton, R., Verdiere, K., Bertolini, C., Bär, R., Groby, J.-P., Geslain, A., Poulain, N., Rouleau, L., Guinault, A., Ahmadi, H., and Forget, C., 2018. “How reproducible are methods to measure the dynamic viscoelastic properties of poroelastic media?”. *Journal of Sound and Vibration*, **428**, pp. 26–43.

[43] Rebillard, P., Allard, J.-F., Depollier, C., Guignouard, P., Lauriks, W., Verhaegen, C., and Cops, A., 1992. “The effect of a porous facing on the impedance and the absorption coefficient of a layer of porous material”. *Journal of sound and vibration*, **156**(3), pp. 541–555.

[44] Veen, J. R., and Saha, P., 2003. Feasibility of a standardized test procedure for random incidence sound absorption tests using a small size reverberation room. Tech. rep., SAE Technical Paper 2003-01-1572.

[45] Veen, J. R., Pan, J., and Saha, P., 2005. Development of a small size reverberation room standardized test procedure for random incidence sound absorption testing. Tech. rep., SAE Technical Paper 2005-01-2284.

List of Tables

1	Models used by each participant to characterise the porous materials of the four tested systems.	7
2	Mechanical and acoustic properties of the considered materials (experimentally evaluated).	8
3	Specification of the software used by each participant.	9

List of Figures

1	Diagram of the Alpha Cabin used for the experimental investigation of the systems: the blue circles represent the position of the three sound sources; the purple circle represents the microphone; the red rectangle is the 1.2 m ² sample.	3
2	Sound absorption coefficient of System #A - comparison between numerical and experimental data: a) the FTMM results are computed considering the finite-size radiation impedance and the angle of incidence in the range $0 \leq \theta \leq \pi/2$; b) comparison between the arithmetic average of the FTMM data and the results computed with some TMM variations.	10
3	Sound absorption coefficient of System #B - comparison between numerical and experimental data: a) the FTMM results are computed considering the finite-size radiation impedance and the angle of incidence in the range $0 \leq \theta \leq \pi/2$; b) comparison between the arithmetic average of the FTMM data and the results computed with some TMM variations.	10
4	Sound absorption coefficient of System #C - comparison between numerical and experimental data: a) the FTMM results are computed considering the finite-size radiation impedance and the angle of incidence in the range $0 \leq \theta \leq \pi/2$; b) comparison between the arithmetic average of the FTMM data and the results computed with some TMM variations.	11
5	Sound absorption coefficient of System #D - comparison between numerical and experimental data: a) the FTMM results are computed considering the finite-size radiation impedance and the angle of incidence in the range $0 \leq \theta \leq \pi/2$; b) comparison between the arithmetic average of the FTMM data and the results computed with some TMM variations.	12
6	Mean difference between the experimental sound absorption coefficient measured in the Alpha Cabin and the results predicted with the FTMM. The error bars represent the standard deviation associated with the arithmetic average of the FTMM results.	13

Accepted Manuscript Not Certified